International Journal of Adhesion & Adhesives 70 (2016) 26–36

Contents lists available at ScienceDirect

International Journal of Adhesion & Adhesives

journal homepage: www.elsevier.com/locate/ijadhadh

Characterizing phenol–formaldehyde adhesive cure chemistry within the wood cell wall

Daniel J. Yelle [a,*], John Ralph [b]

[a] U.S. Forest Products Laboratory, U.S.D.A. Forest Service, 1 Gifford Pinchot Drive, Madison, WI 53726, USA
[b] Department of Biochemistry, DOE Great Lakes Bioenergy Research Center, and Wisconsin Energy Institute, University of Wisconsin, 1552 University Avenue, Madison, WI 53726, USA

ARTICLE INFO

Article history:
Accepted 2 May 2016
Available online 9 May 2016

Keywords:
Adhesives for wood
Phenolic
Wood and wood composites
Adhesion by chemical bonding
Arylglycerol-β-aryl ether

ABSTRACT

Adhesive bonding of wood using phenol–formaldehyde remains the industrial standard in wood product bond durability. Not only does this adhesive infiltrate the cell wall, it also is believed to form primary bonds with wood cell wall polymers, particularly guaiacyl lignin. However, the mechanism by which phenol–formaldehyde adhesive integrally interacts and bonds to lignin within the cell wall remains unclear. We used recently developed solubilization methodologies in conjunction with two-dimensional ^{1}H–^{13}C solution-state NMR spectroscopy of ball-milled pine earlywood and latewood bonded assemblies to characterize the chemical modification of wood cell wall polymers after phenol–formaldehyde curing at various cooking times. The results showed that the highly alkaline resin at 140 °C decreased the frequency of the principal arylglycerol-β-aryl ether interunit linkage by eighty percent in earlywood and by twenty percent in latewood. The presence of newly formed diarylmethanes between guaiacyl lignin units and phenolic methylols was confirmed via NMR spectra of the aliphatic methylene and aromatic regions. The phenol–formaldehyde cure chemistry showed that *o*–*p* methylene bridges dominated in both earlywood and latewood cell walls, but the propensity of *p*–*p* substitution is higher in the latewood cell wall. Our results provide evidence for a simultaneous wood polymer degradation and guaiacyl unit C5 bond formation that occurs during phenol–formaldehyde curing. This competition may be necessary for developing good bond durability between the adhesive and wood.

Published by Elsevier Ltd.

1. Introduction

Phenol–formaldehyde (PF) adhesive dates back to the mid-1930s when it was introduced as the first truly synthetic plywood adhesive. Its performance and durability has been unrivaled and remains a significant mainstay in the wood composite industry. Despite its ubiquitous use, elucidating its adhesion mechanisms with wood has been challenging. Research has confirmed that PF adhesive does indeed infiltrate the wood cell wall [1–7]; however, characterizing how the PF interacts with the cell wall polymers has not been well described. The energy of activation during curing of PF-based adhesives has been repeatedly shown to be lowered in the presence of wood [8–13]. These studies have led researchers to accredit strong primary intermolecular interactions (e.g., covalent linkages) between these adhesives and wood as a contributor to bond durability. The potential for covalent bond formation to occur between PF and wood has been demonstrated [12,14], but evidence also suggests that its contribution may be small under standard thermosetting conditions, and that numerous secondary intermolecular forces between the substrate and PF oligomers may be solely responsible for substrate-induced activation of phenolic reactive sites [15]. However, what still remains quite mysterious is the structural chemistry of the wood cell wall following PF adhesive curing and a knowledge of the extent to which the wood has been chemically modified. With wood cell wall dissolution techniques in conjunction with two-dimensional solution-state NMR spectroscopy [16,17] some important aspects of wood adhesion mechanisms are now becoming evident [18]. Discerning chemical reactivity between adhesives and wood, and which cell wall polymers are involved, is not only important for understanding fundamental wood adhesion mechanisms, but is necessary to advance the field of wood adhesion towards new adhesive technologies, especially those that utilize lignin byproducts as PF resin substitutes.

The mechanism of alkali-catalyzed PF curing is considered by most to be a two-stage reaction. The initial stage consists of phenolate/enolate formation involving resonance-stabilized ions with significant negative charge density at the 2-, 4-, and 6-positions of

* Corresponding author.
E-mail address: dyelle@fs.fed.us (D.J. Yelle).

http://dx.doi.org/10.1016/j.ijadhadh.2016.05.002
0143-7496/Published by Elsevier Ltd.

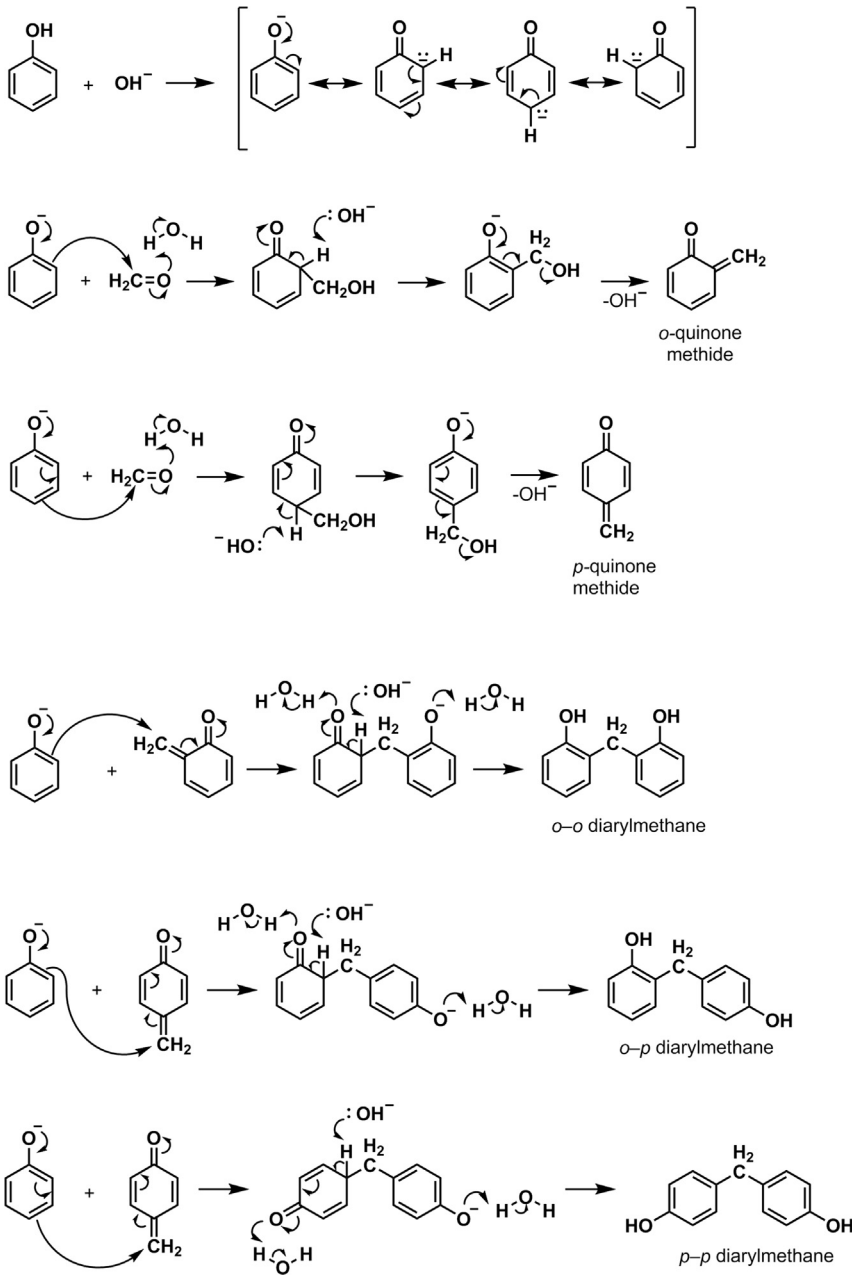

Fig. 1. Alkali-catalyzed reaction of phenol with formaldehyde to form reactive quinone methides that condense with phenol and polymerize to form PF resin.

the phenol followed by methylol formation via nucleophilic attack (S_N2) by the anion onto the formaldehyde carbonyl. During the second stage, the temperature is increased and the resols condense to form methylene bridges via a quinone methide intermediate (Fig. 1) [19].

Lignin, a largely linear polyphenylpropanoid comprising approximately 25–30% of wood polymers, has phenolic endgroups that render it compatible with some applications of phenol. It has the capability of reacting with other phenols and hydroxymethylated phenols during adhesive curing, for example [20].

Studies involving lignin model compounds [21–26] and isolated lignins [20,26–28] have shown that, under alkaline conditions at temperatures ≥ 100 °C, free-phenolic β-aryl ether units release formaldehyde to give vinyl ethers (more appropriately termed styryl ethers, Fig. 2a) [20–25,27,28]. Similarly, free-phenolic phenylcoumaran units release formaldehyde to give stilbenes (Fig. 2b) [26,29–32]; α-ether linkages in phenolic structures can be selectively cleaved with mild alkali treatments at room temperature [33]. Most of the released formaldehyde from styryl ether and stilbene formation may result in methylene bridges between the C5-positions of guaiacyl units (Fig. 2c) to give diarylmethane structures [20,34,35]. Studies by Capanema et al. [36] and Balakshin et al. [37] did not see evidence for guaiacyl–guaiacyl diarylmethanes from biogenic formaldehyde in their analyses of Kraft lignin and Kraft-AQ lignin. The lack of diarylmethanes in their studies may be explained by the fact that the addition of sodium sulfide [38] and anthraquinones [27] in pulping have been shown to dramatically increase the rate of delignification by β-aryl ether cleavage and this cleavage occurs prior to styryl ether formation [27]. Thus, the minor amounts of released formaldehyde during Kraft pulping would not have a chance to condense to form diarylmethanes.

Etherified (i.e., non-phenolic) β-aryl ether units exposed to alkaline conditions and temperatures ≥ 100 °C will result in cleavage of the β-aryl ether linkage via an α,β- or β,γ-epoxide intermediate (Fig. 2d)

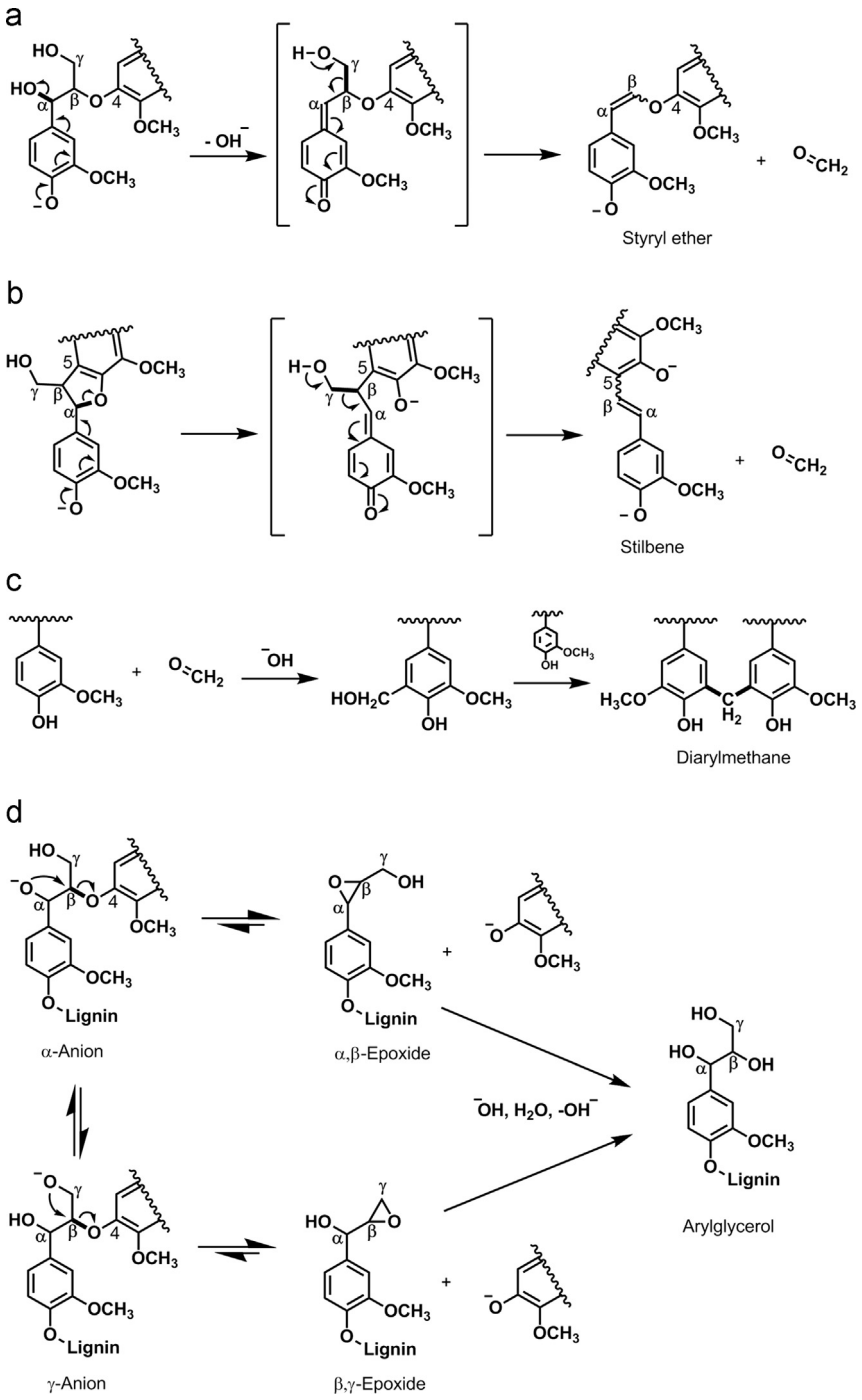

Fig. 2. Lignin hydrolysis of β-aryl ether (a) and phenylcoumaran (b) units, methylene bridge formation via condensation of formaldehyde with free-phenolic units (c), and arylglycerol formation via an epoxide intermediate of non-phenolic β-aryl ether units (d). Bolded bonds highlight those being broken or those that are formed during curing.

[32,39,40]. On the other hand, the α-ether linkages in non-phenolic phenylcoumarans are essentially stable in strong alkali [32].

In this study, the curing chemistry of PF adhesive is characterized within the cell walls of loblolly pine earlywood and latewood. Solution-state NMR spectroscopy of dissolved PF bonded wood sections are analyzed for changes in chemistry using a two-dimensional $^{1}H–^{13}C$-correlation (HSQC) NMR. The hope was to reveal how PF adhesive interacts with itself and with wood cell wall polymers, in part dictated by resin molecular weight and wood growth ring micro/nanopore distribution. For example, the free-volume (i.e., the pore spaces within the cell wall that are not occupied by polymers) in earlywood and latewood from the sapwood of gymnosperms is known to be markedly different [41,42]. Furthermore, NMR identification of newly formed structures either between PF moieties or between PF and native wood polymers, along with elucidating wood cell wall degradation, allows PF cure mechanisms in wood to be delineated to a level where reactivity can be quantified.

2. Experimental procedure

2.1. Microtomed wood preparation

Loblolly pine cubes (20 mm^3) that had tangential sides exactly perpendicular to the radial sides were selected. This was so that,

when sectioning tangentially with the microtome, the sections would be either entirely made up of earlywood or latewood. The cubes were placed in boiling distilled water for 10 min and then kept submerged for 24 h before sectioning. Microtomed wood was prepared using a sled microtome (Spencer Lens Company, Buffalo, NY) to give tangential earlywood and latewood sections (0.030 mm radial × 20 mm tangential × 20 mm longitudinal) and equilibrated to a moisture content of 10% using a chamber in which the moisture content was maintained at that level with a saturated salt (NaBr) solution.

2.2. PF resin formulation and application

Phenol (10.0 g) and formaldehyde (17.9 g of a 37% aqueous solution) were charged into a cooled round bottom flask (5 °C) with stirring. After heating to 25 °C, NaOH (1.1 g, 50%) was added dropwise. The mixture was then heated to 70 °C over 15 min and held for 60 min. After the first cook stage, the second NaOH aliquot (0.6 g, 50%) was added quickly to the reaction flask which was then heated to 85 °C over 15 min. After about 45 min the resin reached the O-P point on the Gardner-Holdt viscosity scale (3.7–4.0 poise). The adhesive was cooled in an ice bath and refrigerated until use.

The reaction was monitored with thin-layer chromatography (TLC) using model compounds and PF standards to follow the stages of polymer growth of the resin at about 30 min increments. At each increment, a 2 mL aliquot was removed from the reaction flask and refrigerated. The increments chosen were at 60, 90, 120, and 150 min, with the 120 min time-point representing a typical PF adhesive for wood composite production (49% solids).

2.3. Molecular weight determination of resins

Gel permeation chromatography (GPC) was used to characterize changes in molecular weight during cooking of the PF resin using a HPLC model 1100 (pump, autosampler, and UV detector) (Agilent, Santa Clara, CA) equipped with an Optilab® T-rEX™ refractive index (RI) detector and a DAWN® HELEOS™ II light scattering detector (Wyatt Technology Corp., Santa Barbara, CA). The ASTRA 6 software (Wyatt Technology Corp., Santa Barbara, CA) was used for data collection and analysis. The column was a Progel™ –TSK G2000 (Sigma-Aldrich, St. Louis, MO) used with HPLC grade *N,N*-dimethylformamide (DMF). PF resin aliquots were dissolved in DMF and filtered through a 0.2 μm PTFE membrane before analysis. Each filtered solution contained a PF resin concentration between 60–80 g/L, and 5 μL of each solution was injected and eluted with DMF at a flow rate of 0.500 mL/min.

2.4. Bondline assembly preparation

Each PF resin time-point aliquot was weighed out onto the wood sections (earlywood or latewood) on an analytical balance so that the weight of the resin solids was approximately twice the weight of the pair of wood sections (i.e., for 25 mg sections, weighed out approx. 100 mg of PF resin, or 50 mg resin solids). The sections were then quickly jointed together on a glass slide; a binder clip held the sections together between two glass slides. The sections (now closed into an assembly) were placed into a non-spouted beaker with a watch glass cover. The sections sat in this closed assembly condition at room temperature for 30 min. The covered assemblies were heated slowly to 140 °C in a small air-sealed oven (over 1 h period) and held for 1 h without air flow to allow for a steam environment. After the sections were fully cooled, they were ready for NMR preparation. In addition to the bonded wood sections, a control PF resin (120 min cook time) was cured alongside the assemblies.

2.5. NMR spectroscopy and analysis

Ball-milling of the PF bonded earlywood and latewood assemblies and controls was done in a Retsch PM100 planetary ball-mill (Newtown, PA) equipped with a 50 mL ZrO_2 jar and using three 20 mm ZrO_2 balls. Initial milling was for 1 h under mild conditions (300 rpm, 10 min pause every 20 min) and followed by 3 h of vigorous milling (600 rpm, 10 min pause every 20 min, ten 10 mm ZrO_2 balls); the jar temperature remained at < 50 °C. One sample (~20 mg) from each milled assembly was directly placed into a 5 mm NMR tube and 500 μL of DMSO-d_6 was added. The sample was sonicated at 30 °C for 1 h.

NMR spectra were acquired at the University of Wisconsin–Madison's Wisconsin Energy Institute, on a Bruker-Biospin (Rheinstetten, Germany) AVANCE 500 MHz spectrometer fitted with a cryogenically cooled 5-mm Bruker TCI (triple resonance cryoprobe optimized for ^{1}H and ^{13}C observation) gradient probe with inverse geometry (^{1}H coils closest to the sample). Heteronuclear Single-Quantum Coherence (HSQC) spectra, where one-bond ^{1}H–^{13}C correlations are obtained, were acquired using an adiabatic pulse sequence [43] 'hsqcetgpsisp2.2' and the following parameters: spectral width from 10 to 0 ppm (5000 Hz) in F2 (^{1}H) using 1998 data points for an acquisition time (AQ) of 200 ms, and interscan delay (D1) of 1.5 s, and from 200 to 0 ppm (25,154 Hz) in F1 (^{13}C) using 400 increments (F1 AQ of 8 ms) of 24 scans, for a total AQ of 4 h 50 min. The $^{1}J_{CH}$ used was 145 Hz. The central solvent peak of DMSO was used as an internal reference for all samples (δ_C 39.51, δ_H 2.49 ppm). Processing of the spectra and peak integrations were conducted using Bruker Biospin's TopSpin software (Mac, v. 3.0). Volume integration of the various contours was performed based on the lignin methoxyl contour as the lignin methoxyl group is believed to be the most stable functionality during alkaline PF curing [44]. The processing used typical matched Gaussian apodization in the ^{1}H dimension and squared cosine-bell apodization in the ^{13}C dimension. Prior to Fourier transformation, the data matrices were zero-filled to 1024 points in the ^{13}C dimension.

3. Results and discussion

3.1. Curing strategy

The curing process of PF resin is initiated during the PF cook and the resin continues to build molecular weight and, once applied to wood, develop interpenetrating polymer networks during each stage of wood panel production. The temperatures used to cure PF-bonded southern pine plywood are typically in the range of 140 °C to 160 °C. Even though industrially produced plywood is hot-pressed in a matter of minutes, heat transfer from the face to the core layers is not immediate and depends largely on panel thickness. After hot-pressing, the curing process continues during hot-stacking (post-cure), which may be several hours [45]. In this study, our intention was to incorporate some of these industrial elements. To obtain a complete cure of the PF resin aliquots in the wood, the temperature of the PF-wood assemblies were slowly heated to 140 °C in an environment that allowed steam to remain localized around the assembly and simulate gradual heat transfer, followed by a hold-time of 1 h at 140 °C to simulate the span of time and temperature used during hot-pressing and hot-stacking.

3.2. Resin molecular weight determination

Three PF resin aliquots (60, 90, and 120 min cook times) were run through the GPC for molecular weight determination; the

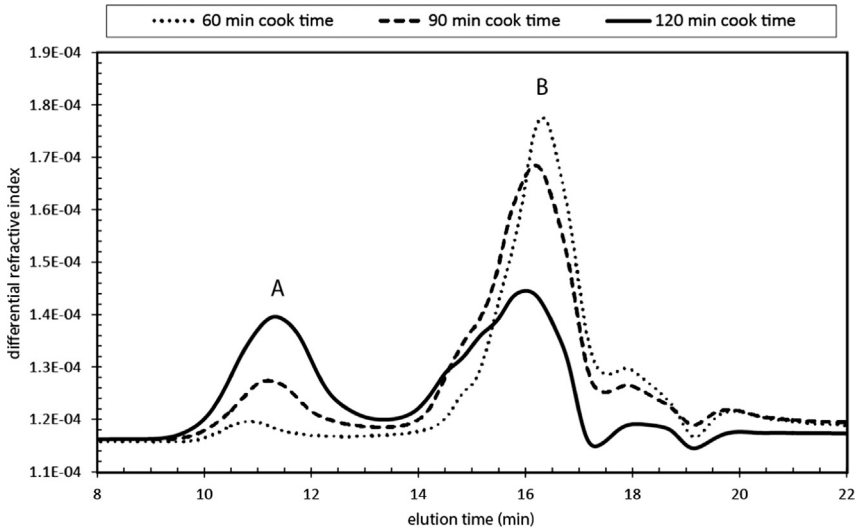

Fig. 3. Molecular weight distributions of the PF resin cook-time aliquots, where peak A represents the higher molecular weight components and peak B the lower molecular weight components.

Table 1
Molecular weights of PF resins with different cook times as analyzed by GPC.

Cook time (min)	Peak	Mass fraction (%)	M_n (g/mol)	M_w (g/mol)	M_w/M_n
60	A	4.7	4120	10,000	2.43
	B	95.3	410	480	1.17
90	A	16.8	12,580	17,340	1.38
	B	83.2	970	1590	1.64
120	A	41.2	52,820	187,300	3.55
	B	58.8	3310	6210	1.88

150 min cook time aliquot was not analyzed because of its insolubility in the elution solvent. The chromatograms (based on the RI data) show two distinct molecular weight groupings, with the higher molecular weights eluting between 10.0 and 13.0 min and the lower molecular weights between 14.0 and 17.5 min (Fig. 3). Table 1 summarizes the results from the molecular weight analysis, where peak A represents the higher molecular weights and peak B the lower molecular weights. It is evident that at the 60 min cook time, 95% of the resin comprises of low molecular weight phenolic methylols that include dimers, trimers, and oligomers. As the cook progressed from 60 min to 90 min to 120 min, a fraction of low molecular weight methylols were converted to highly condensed polymeric structures containing methylene bridges between phenolic groups, with masses of high molecular weight fractions of 5%, 17%, and 41%, respectively. The condensation reactions increased in number and rate such that once past 90 min the molecular weight increased substantially; for example, at the 90 min and 120 min cook times, peak A shows that M_n and M_w increased four-fold and eleven-fold.

3.3. Formaldehyde released from lignin

Under alkaline conditions, the free-phenolic β-aryl ether and phenylcoumaran units are known to cleave at the C_β–C_γ bond (via a retro-aldol reaction); formaldehyde is released from the quinone methide intermediate to give the styryl ether and stilbene structures (Fig. 2). Hydrolysis of a 4–O-bond will also occur to a certain degree under these conditions, resulting in a new phenolic from a previously etherified unit. Previous literature of a styryl ether model compound showed NMR correlations for Hα/Cα and Hβ/Cβ (*cis*) to be 6.2/112.5 and 7.3/143.0 ppm and for Hα/Cα and Hβ/Cβ (*trans*) to be 5.6/109.5 and 7.3/145.2 ppm, respectively [35,37,46–48]. Fig. 4 shows the aromatic regions of the HSQC spectra from both the earlywood and latewood assemblies that were bonded with the 120 min cook time PF resin. Styryl ether correlations are not present in the earlywood-PF spectrum (Fig. 4a), whereas, in the latewood-PF spectrum (Fig. 4b), there are correlations that are consistent with *cis*-styryl ethers. For example, these *cis*-isomer correlations 6.11/112.8 and 7.46/142.1 ppm are present in all of the latewood-PF spectra. Correlations consistent with the *trans*-isomer were present only in the latewood-PF spectra at 5.65/109.0 and 7.35/147.0 ppm, but as very weak contours (data not shown). The amount of styryl ethers present in the latewood PF assemblies is not substantial. Dimmel and Bovee [46] demonstrated that, under alkaline pulping conditions, styryl ether model compounds were slowly hydrolyzed only when the temperatures reached 170 °C, and that at 150 °C the styryl ether did not degrade and was in equilibrium with the quinone methide. As the PF curing temperature used in this present study was 140 °C and there was a low amount of styryl ethers found in the PF bonded assemblies, styryl ether degradation may have occurred due to the high NaOH concentration in the PF resin, as was observed under alkaline pulping conditions with lignin models [49,50]. For example, our synthesized PF resin contains 0.06% NaOH (0.85 g NaOH/14.5 g total resin solids). Therefore, for each 0.025 g assembly there is 0.006 g (0.00015 mol) of NaOH present. The loblolly pine used in this study contains approximately 30% lignin [18], giving 0.0075 g lignin per assembly. If β-aryl ethers are approximately 1006 μmol/g of pine lignin [51], then there are approximately 7.5 μmoles of β-aryl ethers per assembly. This means that for every 1 mol of β-aryl ether in the assembly, approximately 20 M equivalents of NaOH are present. At this high NaOH concentration, it is likely that degradation of styryl ethers occurred during the PF curing process, and the HSQC spectra reflect an underrepresentation of their initial formation.

The NMR of stilbene structures, via analogous retro-aldol reactions of free-phenolic phenylcoumarans, has also been studied previously [36,37,52,53]. They typically show correlations of 7.1–7.4/128.5 ppm for both Hα/Cα and Hβ/Cβ, but do tend to overlap with some other lignin aromatics. In our case, these correlations, if present, would overlap with the existing aromatic condensed units (e.g., approx. 7.0–7.5/130 ppm) formed via PF resin polymerization. Thus, stilbene correlations were not able to be confirmed with these HSQC experiments.

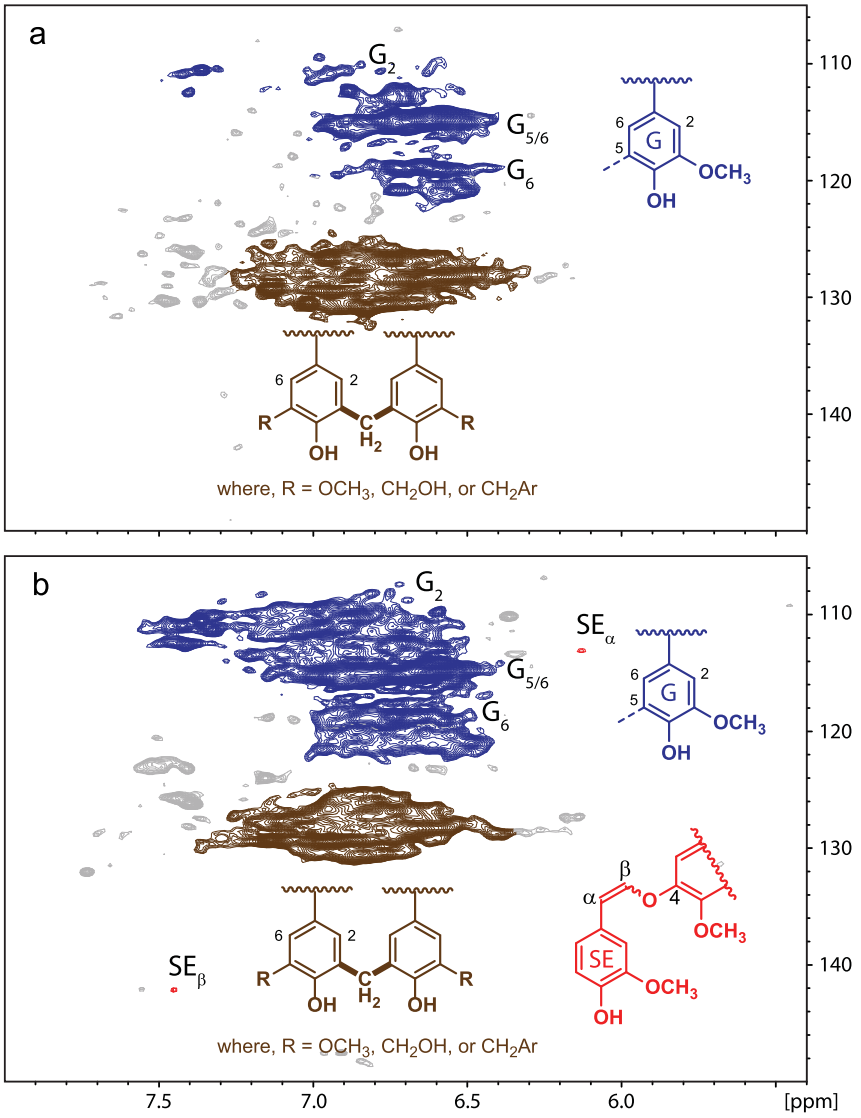

Fig. 4. The aromatic region of NMR ^{1}H–^{13}C correlation spectra showing: earlywood (a), and latewood (b) cured with 120 min cook-time PF resins. The native guaiacyl correlations are blue and the 2/6-position correlations (*meta* to the phenolic hydroxyl) of the diarylmethane structures (containing the methylene bridge) are brown. The (*cis*) styryl ether correlations (red) are only seen (at low levels) in the latewood assemblies. (For interpretation of the references to color in this figure legend, the reader is referred to the web version of this article.)

3.4. Aromatic condensed units

When studying the kinetics of producing methylolated phenol from phenol with formaldehyde, the *para* position has a somewhat greater reactivity with formaldehyde than the *ortho* position (i.e., k_0=6.2 vs k'_0=10.5) [54]. However, once a methylol group is introduced, the remaining positions become less reactive. For example, they found that the reaction rate of *p*-methylol phenol → 2,4-dimethylol phenol was 7.5, whereas that of *o*-methylol phenol → 2,6-dimethylol phenol was 8.7. It would then be logical to see a slightly greater number of *para*-methylolated phenols within the PF adhesive. To get a quantitative sense for this, volume integration was performed (Table 2) on the *para*-substituted methylol (4.51/59.8 ppm) and the *ortho*-substituted methylol (4.49/59.3 ppm) [55,56] contours in the HSQC spectra of PF bonded earlywood and latewood. From these integral data, the *para*-methylols are approximately twice as frequent as the *ortho*-methylols in the cured PF-wood bondlines. As these methylols were found in the cured adhesive, many methylols remained free and did not crosslink, indicating that their quinone methide derivatives were either not formed at a significant rate or were not accessible to attack by a phenolate.

The methylene bridge (aryl–CH_2–aryl) is the predominant linkage formed between PF resins as well as, potentially, the guaiacyl units in lignin. During the second phase of alkaline PF polymerization (i.e., condensation), the phenolate moiety has three resonance forms (Fig. 1) that can thus lead to three different methylene bridge scenarios via an adjacent quinone methide moiety: *ortho–ortho* (*o–o*), *ortho–para* (*o–p*), and *para–para* (*p–p*). The methylolated PF resin can be thought of as a pre-polymer that can be fully cured upon heat. As the resin aliquots are predominantly based upon *para*-substituted methylols, the predominant methylene bridges should be *o–p* and *p–p*. Fig. 5 shows spectra of the aliphatic methylene bridge region for the earlywood cured with PF, latewood cured with PF, and the cured PF itself. The relative ratios of the *o–p* and *p–p* methylene bridge structures may vary based upon the amount of free-volume available in the earlywood and latewood cell walls during the PF curing process. It is clear that both the earlywood PF and latewood PF bonded assemblies show a predominance of *o–p* methylene bridges at 3.67/34.7 ppm (Fig. 5a and b). However, the latewood PF bonded assemblies show a definite increase in propensity for *p–p* methylene bridges at 3.57/39.7 ppm (Fig. 5b). This phenomenon is interesting because the PF cure mechanism is

Table 2
Volume integrals of contours in the HSQC NMR spectra to quantify PF curing chemistry relative to lignin methoxyls*.

Structure	EW control	LW control	EW PF 60 min cook	EW PF 90 min cook	EW PF 120 min cook	EW PF 150 min cook	LW PF 60 min cook	LW PF 90 min cook	LW PF 120 min cook	LW PF 150 min cook
Aα	0.079	0.083	nd	0.023	0.015	0.015	0.064	0.061	0.062	0.073
Bα	0.018	0.020	nd	nd	nd	nd	0.007	0.007	0.011	0.014
Lignin (G_2)	0.174	0.178	nd	0.086	0.075	0.091	0.158	0.142	0.155	0.188
4-*O*-MeGlcA	0.009	0.017	nd	0.006	nd	0.005	0.017	0.016	0.017	0.017
o–o –CH_2–	–	–	0.076	0.042	0.049	0.024	0.007	0.004	0.003	nd
o–p –CH_2–	–	–	0.174	0.120	0.149	0.125	0.052	0.038	0.036	0.028
p–p –CH_2–	–	–	0.085	0.047	0.125	0.045	0.036	0.021	0.022	0.020
o–p/p–p	–	–	2.053	2.582	3.176	2.798	1.473	1.809	1.617	1.349
o–o/p–p	–	–	0.899	0.907	1.053	0.537	0.201	0.208	0.146	–
o–p/o–o	–	–	2.283	2.846	3.015	5.209	7.322	8.716	11.092	–
total –CH_2–	–	–	0.334	0.209	0.245	0.193	0.095	0.064	0.062	0.048
o-methylol	–	–	nd	0.006	nd	nd	0.037	0.017	0.013	0.017
p-methylol	–	–	0.062	0.012	0.017	nd	0.068	0.024	0.027	0.039
total methylol	–	–	0.062	0.018	0.017	nd	0.105	0.042	0.040	0.056
–CH_2–/methylol	–	–	5.409	11.917	14.878	–	0.908	1.543	1.556	0.856
PF aromatics	–	–	4.000	1.749	2.382	2.000	0.797	0.560	0.510	0.436

nd = none detected

* Based on the lignin methoxyl group contour. Note that absolute quantitation is not currently possible, but that comparative integrals reflect the relative amounts of individual components.

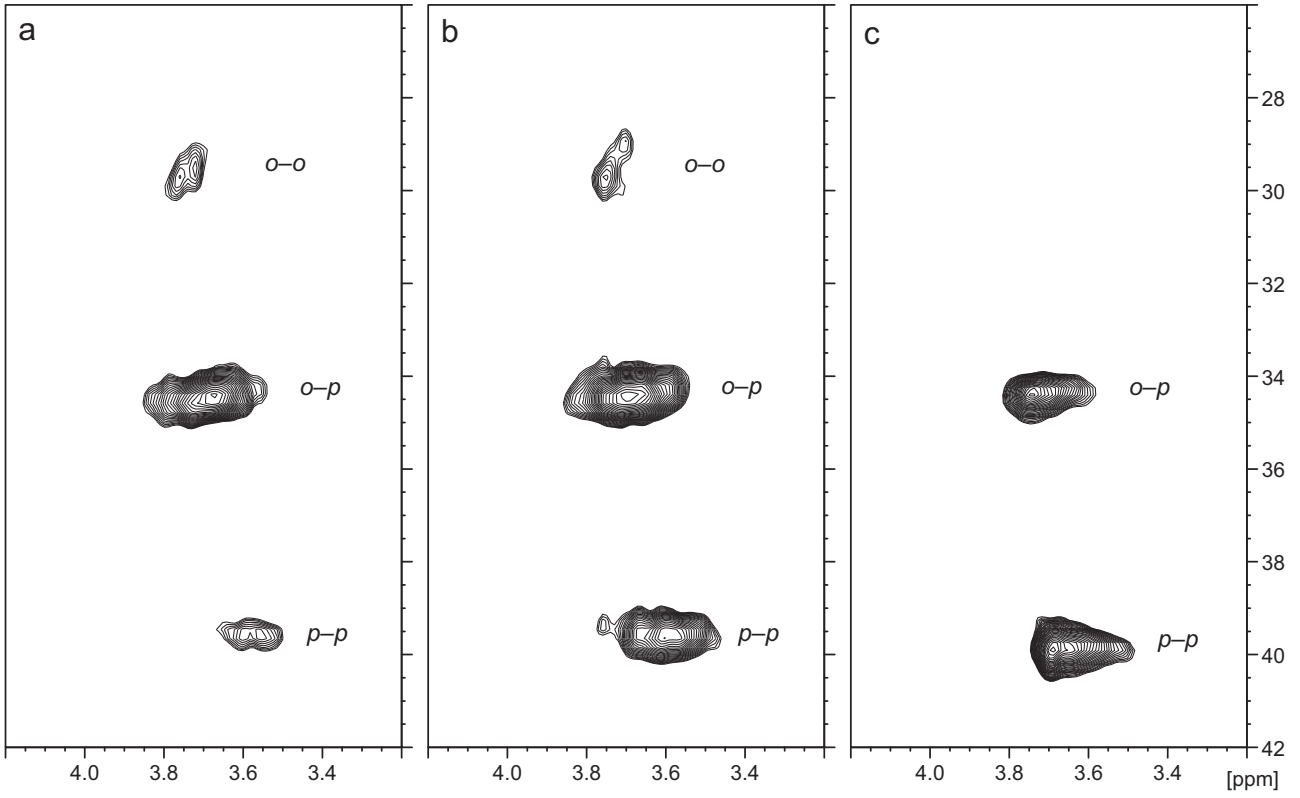

Fig. 5. Partial HSQC spectra of the aliphatic region from the 120 min cook time PF cured with earlywood (a), the 120 min cook time PF cured with latewood (b), and the cured 120 min cook time PF (c). The spectra display methylene correlations for *ortho–ortho*, *ortho–para*, and *para–para* diarylmethanes.

seemingly being partially directed by the free-volume in which the polymer has to work. The cure mechanism in earlywood tends to favor more *o–p* substitution of the PF adhesive, whereas the latewood tends to incorporate more *p–p* substitution compared to the earlywood, possibly due to steric hindrances in the more constrained micro/nanopores of the latewood cell wall. By integrating these methylene bridge NMR contours, shown in Table 2, it can be seen that when PF is bonded with earlywood, the *o–p/p–p* ratio is on average 2.7 vs an average of 1.6 with latewood. Furthermore, the *o–o/p–p* ratio decreases approximately four-fold going from earlywood (average of 0.85) to latewood (average of 0.19), confirming the formation of more *p–p* methylene bridges in the latewood.

To better understand the amount of crosslinking that occurred during the PF-wood curing process, the total amount of methylene bridge formation was compared to the total amount of methylol formation using integration data from Table 2. The earlywood bonded assemblies contain a higher amount of methylene bridges (e.g., the 120 min cook time gave 14 times more methylene bridges

than free methylols in the earlywood). However, in the latewood bonded assemblies the ratio of methylene bridges to free methylols drops to approximately 1.5. This result once again suggests that cell wall pore size has a definite effect on the PF curing chemistry. The latewood cell wall, because of its smaller pore size environment, seemingly does not allow for as much crosslinking of the PF adhesive when compared to the earlywood.

o-Methylol-phenols originating from PF resin and (wood-derived plus added) formaldehyde are not the only source of *o*-quinone methides during PF bonding with wood. As was briefly introduced, free-phenolics are present in lignin as well and their levels increase during alkaline hydrolysis from fragmentation of free-phenolic β-aryl ethers to produce styryl ethers and a new phenolic end-unit on the polymer [27,50]. The C5 position on a free-phenolic guaiacyl end-unit is the only position available for methylol formation under alkaline conditions, giving an *o*-methylol guaiacyl unit that could then condense with phenol, methylolated phenols and, hypothetically, other guaiacyl end-units. The *o*-methylol guaiacyl unit reactivity depends not just on kinetics, but also on sterics and how intimately the units come into contact with phenol. As the PF resin cures and becomes more sterically hindered, the surrounding lignin moieties become a more likely point of contact and, thus, increase their potential for reaction. According to the literature, the NMR chemical shifts of the methylene bridges between a guaiacyl unit and another guaiacyl unit (i.e., to give a *o*–*o* diarylmethane) are quite similar to those of the methylene bridges between PF phenolic units [34,35,47]. Several model compound studies have revealed some slight differences in chemical shifts of the methylene bridge when methoxyls are present on the aromatic ring [47,57–60]. With the current study, we can see some distinctions when analyzing the HSQC spectra. For example, the cured neat PF correlations in the aliphatic region show predominantly *o*–*p* and *p*–*p* methylenes at 3.75/34.3 ppm and 3.70/39.8 ppm, respectively (Fig. 5c); the *o*–*o* methylene (3.75/29.5 ppm) is barely present and not shown here due to its low intensity. These *o*–*p* and *p*–*p* correlations from cured PF are in the same vicinity as in the PF cured earlywood and PF cured latewood spectra (Fig. 5a and b), but the fairly strong *o*–*o* correlations—3.75/29.8 and 3.71/29.7 ppm in the PF cured earlywood, and 3.74/29.9 and 3.70/29.1 ppm in the PF cured latewood—strongly suggest methylene bridge formation other than from curing of the PF resin itself, namely methylene bridges involving a guaiacyl unit from lignin. Furthermore, if guaiacyl C5 positions are methylolated and condensed, the C5 would convert from a tertiary carbon to a quaternary carbon (unprotonated), which influences the chemical shift of the H6/C6 position (*meta* to the phenolic hydroxyl) of that ring. Fig. 6 compares the aromatic region of loblolly pine earlywood, loblolly pine latewood, loblolly pine

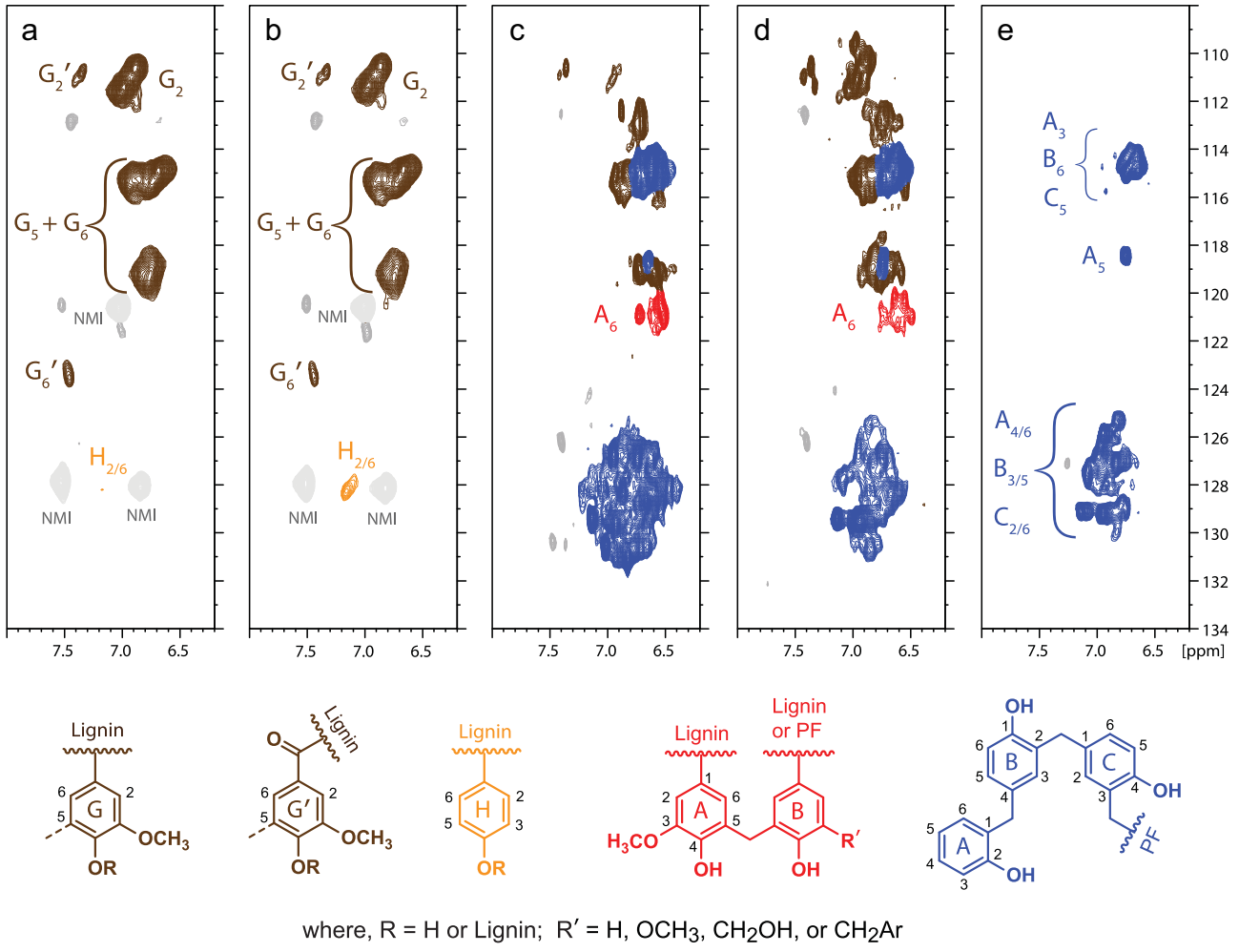

Fig. 6. Partial HSQC spectra of the aromatic region from: loblolly pine earlywood (a), loblolly pine latewood (b), the 120 min cook time PF cured with earlywood (c), the 120 min cook time PF cured with latewood (d), and the cured 120 min cook time PF alone (e). The brown contours are from guaiacyl units (**G**), the blue contours are from PF moieties, and the red contours denote correlations that have chemical shifts consistent with the A6 positions in lignin guaiacyl units adjacent to a methylene bridge at A5. The NMI (gray) peaks are from N-methylimidazole, which was used in the dissolution. (For interpretation of the references to color in this figure legend, the reader is referred to the web version of this article.)

earlywood cured with PF, loblolly pine latewood cured with PF, and cured PF adhesive alone. The H5/C5 correlation for free-phenolic guaiacyl lignin units in loblolly pine is shown at 6.74/114.7 ppm, whereas its H6/C6 correlation is at 6.82/119.2 ppm. From the spectra of loblolly pine earlywood and latewood cured with PF (Fig. 6c and d), the H5/C5 correlation for free-phenolic lignin is overlapped with cured PF correlations, making this difficult to interpret. However, new contours have emerged centered around 6.62/120.9 ppm that are assigned to new guaiacyl unit H6/C6 correlations that have shifted upfield in response to the adjacent methylene bridge at C5 [59]. This new contour gives supporting evidence that free-phenolic lignin units react at their C5 positions to form methylene bridges between phenol, methylolated phenol, or another guaiacyl unit at C5.

3.5. Depletion of native structures

If a particular linkage from a native polymer is cleaved, we would see a depletion of this linkage via the HSQC spectra. The cleaved unit may become sequentially cleaved further to result in low molecular weight compounds, and/or it could be reacted with another polymer/molecule. The native lignin linkages include: β-aryl ethers **A**, phenylcoumarans **B**, and pinoresinols **C**. Fig. 7 shows typical HSQC spectra of the sidechain region of earlywood and latewood loblolly pine cell walls along with representative spectra of the PF-wood cured assemblies. It was evident from the integral data in Table 2 that the most severe depletion of lignin was seen with the PF-bonded earlywood in the 60 min cook-time assembly, where the lowest molecular weight PF was bonded; all of the **A**, **B**, and **C** structures (as well guaiacyl units, G2) were modified to such a degree that their typical chemical shifts have been rendered absent. This modification, via alkaline hydrolysis, may have increased the susceptibility of the cell wall to infiltration of alkali at the earlier stages of PF methylol formation. It was not until the 90 min cook-time assembly, in the early PF polymerization stages, that some of structure **A** remained unmodified in the PF-bonded earlywood, showing that alkaline hydrolysis is lessened potentially due to less alkali present and a decreased chance for mobile compounds to enter the cell wall due to entrapment in the growing polymer. However, these spectra show that even though the higher molecular weight components of PF resin are filtered out of the earlywood cell wall, the alkali will infiltrate beyond that of the PF resin and continue to hydrolyze wood polymers to a certain degree. For example, in the PF-bonded earlywood, structure **A** (Aα, 4.73/71.0 ppm) was depleted approximately 75% in the 90 min, 120 min, and 150 min cook time assemblies. As no styryl ethers were detected in the PF-bonded earlywood assemblies, one possible scenario for such a dramatic decrease in structure **A** is that if most of the β-aryl ethers are non-phenolic and that the alkali concentration was higher than 1 M—the concentration normally seen under alkaline pulping conditions. Gierer and Ljunggren [21] observed a high yield of guaiacol (80%) from lignin model systems using 4 M alkali at 145 °C, giving support to the cleavage of non-phenolic β-aryl ethers via the epoxide mechanism shown in Fig. 2d. Therefore, the fact that we saw no styryl ethers in the PF-bonded earlywood spectra, the β-aryl ethers most likely cleaved before they could form styryl ethers. The complete disappearance of structure **B** (Bα, 5.47/87.0 ppm) in the PF-bonded

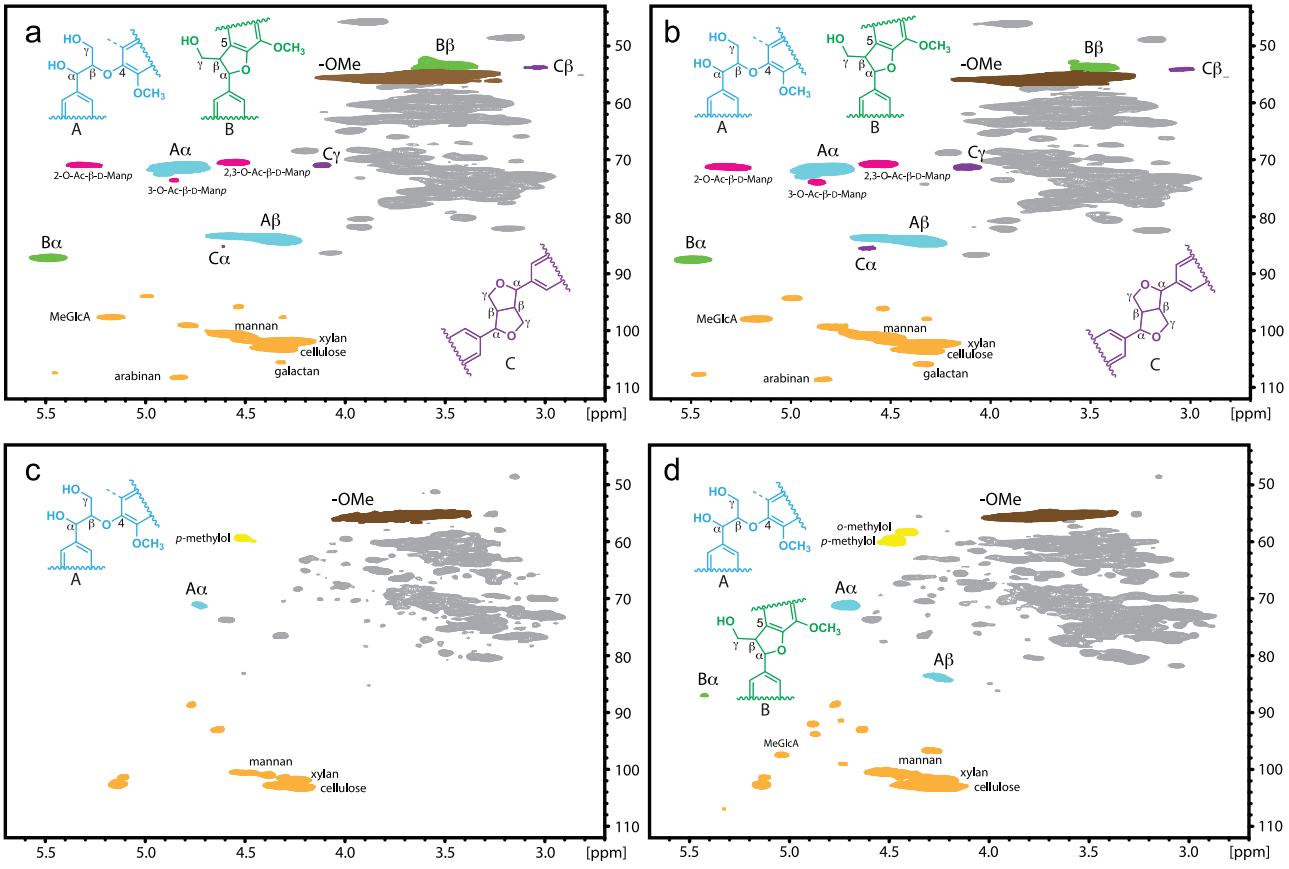

Fig. 7. Partial HSQC spectra showing the sidechain regions for: loblolly pine earlywood (a), loblolly pine latewood (b), 120 min cook time PF cured with earlywood (c), and 120 min cook time PF cured with latewood (d). The labels correspond to the following: phenolic methylols (yellow); β-aryl ethers (structure **A**, cyan); phenylcoumarans (structure **B**, green); pinoresinols (structure **C**, purple); lignin methoxyl (brown); 2-*O*-, 3-*O*-, and 2,3-*O*-acetylated (galactogluco)mannan units (magenta); polysaccharide anomerics (orange); polysaccharide sidechain structures (gray). (For interpretation of the references to color in this figure legend, the reader is referred to the web version of this article.)

earlywood assembly HSQC spectra suggests that most of the phenylcoumarans are likely phenolic, thus cleaving the α-ether and converting to stilbene structures (Fig. 2b), as these α-ethers are highly susceptible to even mild alkaline conditions [32,33].

With the PF-bonded latewood assemblies, the depletion of the **A**, **B**, and **C** structures was much lessened, suggesting that the smaller pore sizes in the latewood tissue may somewhat limit PF resin and alkali infiltration into the cell wall matrix. For example, structure **A** (Aα, 4.71/71.1 ppm) was depleted approximately 25% in the 60 min, 90 min, 120 min cook time assemblies; the 150 min cook time assembly display only minor structure **A** depletion. This lessened affect was also observed by the low depletion of structure **B** (Bα, 5.43/86.9 ppm). These results may also suggest potentially different lignin structural chemistries between the earlywood lignin and latewood lignin. For example, unlike the PF-bonded earlywood assemblies, styryl ethers were detected in the PF-bonded latewood assemblies, thus displaying a greater resistance to β-aryl ether cleavage. Since styryl ethers only form with phenolic β-aryl ethers (Fig. 2a), this could mean that the latewood has more phenolic β-aryl ether units than earlywood. Furthermore, the more steadfastness of the phenylcoumarans in the PF-bonded latewood assemblies could mean that phenylcoumarans are more non-phenolic in the latewood as compared to the earlywood.

Polysaccharides, also have a strong potential to react or become modified during the PF-bonding process. Hemicelluloses are highly susceptible to physical and chemical changes in alkali, including swelling, dissolution, precipitation, hydrolysis reactions, and endwise depolymerization reactions (i.e., peeling) [61]. From the appearance of the anomeric region of the spectra (Fig. 7), it appears that the polysaccharides in the earlywood were more heavily degraded and modified than those in the latewood when bonded with PF, especially in the earlier cook-time assemblies. Not only have the cellulose, mannan, xylan, arabinan, and galactan levels decreased due to PF-bonding, but complete removal of the native 2-*O*- and 3-*O*-acetyl groups from mannan units on galactoglucomannan for all PF-bonded assemblies analyzed. Acetyl groups are readily cleaved by alkali, which end up as acetate [62]. Partial removal of the 4-*O*-methyl-α-D-glucuronic acid groups from arabinoglucuronoxylan was also evident from the HSQC spectra (5.05/97.2 ppm) for earlywood PF-bonded assemblies. The glycosidic linkages between the glucuronic acid group and the xylan chain are most likely cleaved via alkaline hydrolysis [62,63]. Another potential reaction is CH_3O elimination at the β-position (C-4) to the carboxyl group, followed by H-5 elimination [64,65].

4. Conclusions

Earlywood and latewood microtomed sections were bonded with alkaline PF resin using selected cook-time aliquots. The bonded assemblies were cured, ball-milled, dissolved, and analyzed using solution-state NMR spectroscopy. 2D ^{1}H–^{13}C-correlation (HSQC) experiments revealed the following: 1. Alkaline hydrolysis of the arylglycerol-β-aryl ether linkages in lignin resulted in a minor amount of *cis*-styryl ethers; 2. The earlywood and latewood PF-bonded assemblies both showed a predominance of *o*–*p* methylene bridges, but the latewood PF-bonded assemblies showed a stronger presence of *p*–*p* methylene bridges, suggesting that wood cell wall micro/nano-scale porosity may influence PF curing chemistry; 3. Reactivity between PF moieties and lignin was evidenced in both the aliphatic methylene region and the aromatic region of the HSQC spectra, showing that lignin C5 positions were partially substituted with PF moieties via methylene bridges; 4. Severity of lignin sidechain and polysaccharide substituent cleavage via alkaline hydrolysis was dependent on the cooking time aliquot used for PF-bonding, with wood bonded with the 60 min cook time aliquot showing the most severe native polymer degradation. This research demonstrates that, during alkaline PF curing with wood, bond formation between PF moieties and lignin occurs simultaneously with wood cell wall polymer degradation and that these mechanisms must compete. It is possible that this competition is one of the underlying explanations for such durable PF bonds with wood. We hypothesize that, as the lignin and polysaccharide matrices degrade under the highly alkaline conditions and temperatures employed here, the lower molecular weight phenol–formaldehyde resin methylol moieties are able to infiltrate the cell wall and form diarylmethanes with phenolates from the resin and those found on guaiacyl units in lignin.

Acknowledgments

We thank Prof. Chip Frazier for very insightful discussions. JR was funded in part by the DOE Great Lakes Bioenergy Research Center (DOE Office of Science BER DE-FC02-07ER64494).

References

[1] Nearn WT. Wood–adhesive interface relations. Off Digest Fed Soc Paint Technol 1965;37:720–33.
[2] Nearn WT. Application of the ultrastructure concept in industrial wood products research. Wood Sci 1974;6:285–93.
[3] Saiki H. The effect of the penetration of adhesives into cell walls on the failure of wood bonding. Mokuzai Gakkaishi 1984;30:88–92.
[4] Smith LA, Côté WA. Studies of penetration of phenol–formaldehyde resin into wood cell walls with the SEM and energy-dispersive X-ray analyser. Wood Fiber 1971;3:56–7.
[5] SEM Gindl W. and UV-microscopic investigation of glue lines in Parallam® PSL. Holz Roh Werkstoff 2001;59:211–4.
[6] Gindl W, Schöberl T, Jeronimidis G. The interphase in phenol–formaldehyde and polymeric methylene di-phenyl-di-isocyanate glue lines in wood. Int J Adhes Adhes 2004;24:279–86.
[7] Jakes J, Hunt C, Yelle D, Lorenz L, Hirth K, Gleber S, et al. Synchrotron-based X-ray fluorescence microscopy in conjunction with nanoindentation to study molecular-scale interactions of phenol-formaldehyde in wood cell walls. ACS Appl Mater Interfaces 2015;7:6584–9.
[8] Mizumachi H, Morita H. Activation energy of the curing reaction of phenolic resin in the presence of woods. Wood Sci 1975;7:256–60.
[9] Proszyk S, Zakrzewski R. Activation energy of curing reaction of phenolic resins in the presence of some selected species of wood. Folia For Pol Ser B 1992;23:101–9.
[10] Horioka K, Gamo M. The mechanism and durability of adhesion in wood glue bonds. In: Proceedings of the IUFRO conference on wood glueing. Madison, WI; 1974. p. 1–40.
[11] Abe I, Tsutsumi K, Yoshimura M. Interaction between wood components and phenol–formaldehyde resins. I. Thermal analysis on saligenin and its cured products. Mokuzai Gakkaishi 1974;20:277–83.
[12] Chow S-Z. Kinetic study of the polymerization of phenol–formaldehyde resin in the presence of cellulosic materials. Wood Sci 1969;1:215–21.
[13] Cherubim M, Henn F. Modellversuche zur Härtung von Phenolharzbindemitteln. Mitt Deut Ges Holzforsch 1971;57:165–74.
[14] Mora F, Pla F, Gandini A. The interactions between wood components and formaldehyde-based resins. I. Monofunctional resin model compounds. Angew Makromol Chem 1989;173:137–52.
[15] Pizzi A, Mtsweni B, Parsons W. Wood-induced catalytic activation of PF adhesives autopolymerization vs. PF/wood covalvent bonding. J Appl Polym Sci 1994;52:1847–56.
[16] Yelle DJ, Ralph J, Frihart CR. Characterization of nonderivatized plant cell walls using high-resolution solution-state NMR spectroscopy. Magn Reson Chem 2008;46:508–17.
[17] Lu F, Ralph J. Non-degradative dissolution and acetylation of ball-milled plant cell walls: high-resolution solution-state NMR. Plant J 2003;35:535–44.
[18] Yelle DJ, Ralph J, Frihart CR. Delineating pMDI model reactions with loblolly pine via solution-state NMR spectroscopy. Part 2. Non-catalyzed reactions with the wood cell wall. Holzforschung 2011;65:145–54.
[19] Megson NJL. Phenolic resin chemistry. New York: Academic Press; 1958. p. 323.
[20] Ekman KH. Formaldehyde obtained by alkaline hydrolysis of wood and lignin. Tappi 1965;48:398–402.
[21] Gierer J, Ljunggren S. Reactions of lignin during sulfate pulping.17. Kinetic treatment of the formation and competing reactions of quinone methide intermediates. Sven Papperstidn 1979;82:503–12.

[22] Miksche G. Über das Verhalten des Lignins bei der Alkalikochung.IX. Zum alkalischen Abbau von Arylglycerin-β-(2,6-dimethoxy-4-alkylaryl)-ätherstrukturen. Acta Chem Scand 1973;27:1355–68.
[23] Gierer J, Lenz B, Wallin N-H. Reactions of lignin during sulfate cooking.V. Model experiments on splitting of aryl–alkyl ether linkages by 2 N sodium hydroxide and by white liquor. Acta Chem Scand 1964;18:1469–76.
[24] Yaguchi T, Hosoya S, Nakano J, Satoh A, Nomura Y, Nakamura M. Mechanism of rapid delignification during alkaline cooking with addition of tetrahydroanthraquinone. Mokuzai Gakkaishi 1979;25:239–40.
[25] Adler E, Falkehag I, Marton J, Halvarson H. The behavior of lignin in alkaline pulping. II. Model experiments with arylalkyl-β-aryl ethers. Acta Chem Scand 1964;18:1313–4.
[26] Marton J, Marton T, Falkehag SI. Alkali-catalyzed reactions of formaldehyde with lignins. In: Marton J, editor. Lignin structure and reactions, 59. Washington, D.C: American Chemical Society; 1966. p. 125–44.
[27] Obst JR, Landucci LL, Sanyer N. Quinones in alkaline pulping. β-ether cleavage of free phenolic units in lignin. Tappi 1979;62:55–9.
[28] Freudenberg K. Die Herkunft des Formaldehyds aus dem Lignin. Chem Ber 1947;80:149–58.
[29] Adler E, Marton J, Falkehag I. The behavior of lignin in alkaline pulping. I. Model experiments with phenylcoumarans. Acta Chem Scand 1964;18:1311–2.
[30] Falkehag I. Stilbene structures in sulphate lignin. Pap Puu 1961;43:655–6.
[31] Wallis AFA. The alkaline hydrolysis of some lignin model 2-arylcoumarans. Aust J Chem 1972;25:1529–35.
[32] Gierer J, Norén I. Über die Reaktionen des Lignins bei der Sulfatkochung.II. Modellversuche zur Spaltung von Aryl-alkylätherbindungen durch Alkali. Acta Chem Scand 1962;16:1713–29.
[33] Adler E, Miksche GE, Johansson B. Über die Benzyl-arylätherbindung im Lignin. I. Freilegung von phenolischem Hydroxyl in Ligninpräparaten durch Spaltung leicht hydrolysierbarer Alkyl–arylätherstrukturen. Holzforschung 1968;22:171–4.
[34] Yasuda S, Yoon B-H, Terashima N. Chromophoric structures of alkali lignin. IV. Chromophoric structures of condensation products from guaiacylglycerol-β-aryl ether [γ–^{13}C]. Mokuzai Gakkaishi 1980;26:421–5.
[35] Landucci LL. Search for lignin condensation reactions with modern NMR techniques. In: Hemingway RW, Conner AH, Branham SJ, editors. Adhesives from renewable resources. Washington, D.C: American Chemical Society; 1989. p. 27–42.
[36] Capanema EA, Balakshin MY, Chen C-L, Gratzl JS, Gracz H. Structural analysis of residual and technical lignins by ^{1}H–^{13}C correlation 2D NMR-spectroscopy. Holzforschung 2001;55:302–8.
[37] Balakshin MY, Capanema EA, Chen C-L, Gracz HS. Elucidation of the structures of residual and dissolved pine kraft lignins using an HMQC NMR technique. J Agric Food Chem 2003;51:6116–27.
[38] Gierer J, Lenz B, Wallin N-H. The splitting of aryl-alkyl ether bonds in milled wood lignin by white liquor. Part VII of a series of the reactions of lignin during sulfate cooking. Tappi 1965;48:402–5.
[39] Gierer J, Kunze I. Zur Spaltung von β-Hydroxy-alkyl-aryläthern durch Alkali. Acta Chem Scand 1961;15:803–7.
[40] Miksche G. Über das Verhalten des Lignins bei der Alkalikochung.VII. Zum alkalischen Abbau der p-Alkoxy-arylglycerin-β-arylätherstrukturen des Lignins. Versuche mit erythro-Veratrylglycerin-β-guajacyläther. Acta Chem Scand 1972;26:3275–81.
[41] Grigsby W, Kroese H, Dunningham E. Characterisation of pore size distributions in variously dried Pinus radiata: analysis by thermoporosimetry. Wood Sci Technol 2013;47:737–47.
[42] Yin J, Song K, Lu Y, Zhao G, Yin Y. Comparison of changes in micropores and mesopores in the wood cell walls of sapwood and heartwood. Wood Sci Technol 2015;49:987–1001.
[43] Kupče E, Freeman R. Compensated adiabatic inversion pulses: broadband INEPT and HSQC. J Magn Reson 2007;187:258–65.
[44] Gierer J, Lenz B, Norén I, Soderberg S. Reactions of lignin during sulfate cooking III. The splitting of aryl-aryl-ether bonds in milled wood lignin by alkali. Tappi 1964;47:233–9.
[45] Sellers, Jr. T. Plywood and adhesive technology. New York: Marcel Dekker, Inc; 1985. p. 680.
[46] Dimmel DR, Bovee LF. Pulping reactions of vinyl ethers. J Wood Chem Technol 1993;13:583–92.
[47] Kringstad KP, Mörck R. ^{13}C-NMR spectra of kraft lignins. Holzforschung 1983;37:237–44.
[48] Yasuda S, Yoon B-H, Terashima N. Chromophoric structures of alkali lignin. III. Chromophoric structures of condensation products from guaiacylglycerol-β-aryl ether [α–^{13}C]. Mokuzai Gakkaishi 1979;25:771–6.
[49] Obst JR, Sanyer N. Effect of quinones and amines on the cleavage rate of β-O-4 ethers in lignin during alkaline pulping. Tappi 1980;63:111–4.
[50] Dimmel DR, Perry LF. Structural/reactivity studies (I): soda reactions of lignin model compounds. Appleton, WI: The Institute of Paper Chemistry; 1985. p. 1–32.
[51] Rolando C, Monties B, Lapierre C. Thioacidolysis. In: Lin SY, Dence CW, editors. Methods in lignin chemistry. Heidelberg, Germany: Springer; 1992. p. 334–49.
[52] Liitiä TM, Maunu SL, Hortling B, Toikka M, Kilpeläinen I. Analysis of technical lignins by two- and three-dimensional NMR spectroscopy. J Agric Food Chem 2003;51:2136–43.
[53] Gierer J, Lindeberg O. Studies on the condensation of lignins in alkaline media.3. Formation of stilbenes, arylcoumarans and diarylmethanes on treatment of spruce wood meal with alkali and white liquor in the presence of xylenols. Acta Chem Scand Ser B 1979;33:580–2.
[54] Freeman JH, Lewis CW. Alkaline-catalyzed reaction of formaldehyde and the methylols of phenol; a kinetic study. J Am Chem Soc 1954;76:2080–7.
[55] Werstler DD. Quantitative ^{13}C n.m.r. characterization of aqueous formaldehyde resins: 1. Phenol-formaldehyde resins. Polymer 1986;27:750–6.
[56] Holopainen T, Alvila L, Rainio J, Pakkanen TT. Phenol–formaldehyde resol resins studied by ^{13}C-NMR spectroscopy, gel permeation chromatography, and differential scanning calorimetry. J Appl Polym Sci 1997;66:1183–93.
[57] Kratzl K, Wagner I. Modellversuche zur Kondensation des Lignins. 2. Mitt. Zur vollständigen Methylierung von Ligninen und Modellen; über Kondensationsreaktionen von Phenolen mit Formaldehyd und Xylose. Holzforsch Holzverwert 1972;24:56–61.
[58] Xi F, Reeve DW, McKague AB. The synthesis and chemical structures of tetrameric lignin model compounds. J Wood Chem Technol 1996;16:35–46.
[59] Ralph SA, Ralph J, Landucci LL. NMR database of lignin and cell wall model compounds. ⟨https://www.glbrc.org/databases_and_software/nmrdatabase/⟩; 2004.
[60] Griggs BF. Modification of Kraft lignins by sulfomethylation and oxidative sulfonation: structure and mechanisms. Raleigh, North Carolina: North Carolina State University; 1985.
[61] Rydholm SA. Pulping processes. New York: Interscience Publishers; 1965. p. 1269.
[62] Sjöström E. Wood chemistry. fundamentals and applications. Second ed.. San Diego, CA: Academic Press, Inc.; 1993. p. 293.
[63] Meier H. On the behaviour of wood hemicelluloses under different pulping conditions. 2. Spruce hemicellulose. Sven Papperstidn 1962;65:589–94.
[64] Johansson MH, Samuelson O. Alkaline destruction of birch xylan in the light of recent investigations of its structure. Sven Papperstidn 1977;80:519–24.
[65] Clayton DW. The alkaline degradation of some hardwood 4-O-methyl-D-glucuronoxylans. Sven Papperstidn 1963;66:115–24.